

Supporting Information for

An In-Situ Formed Tunneling Layer Enriches the Options of Anode for Efficient and Stable Regular Perovskite Solar Cells

Xuesong Lin¹, Yanbo Wang^{1,*}, Hongzhen Su¹, Zhenzhen Qin¹, Ziyang Zhang¹, Mengjiong Chen¹, Min Yang¹, Yan Zhao¹, Xiao Liu², Xiangqian Shen¹, Liyuan Han^{1,2,*}

¹State Key Laboratory of Metal Matrix Composites, Shanghai Jiao Tong University, Shanghai 200240, P. R. China

²Special Division of Environmental and Energy Science, Komaba Organization for Educational Excellence, College of Arts and Sciences, University of Tokyo, Tokyo 153-8902, Japan

*Corresponding authors. E-mail: han.liyuan@sjtu.edu.cn (Liyuan Han); sjtu-wyb@sjtu.edu.cn

(Yanbo Wang)

Note S1: Key Parameters Affecting PCE in Regular Ag-PSCs

The influence of each parameter (P) by dark storage on the PCE of devices be evaluated by an improvement index (ΔI), as shown in Eq. S1. After 48h stored under dark and dry environment, the PCE showed a ΔI of 25.3%, with ΔI s of 1.4%, 0.5% and 22.8% for V_{OC} , J_{SC} and FF, respectively. Moreover, the FF as the key parameters affecting PCE was enhanced mainly by the halved R_s (Fig. S2E), which normally related to the improvement of interface charge transport and collection. As shown in Fig. S1, the first 24 h for storage was critical in which period the major improvement of PCE happened.

$$\Delta I = \frac{P(48h-f)+P(48h-r)-P(0h-f)+P(0h-r)}{P(0h-f)+P(0h-r)} \quad (S1)$$

In detail, when we consider the solar cell system as an equivalent circuit with parasitic resistance (Fig. S2A), the parasitic resistance includes R_s and R_{sh} , and the volt-ampere characteristics can be described by Eq. S2.

$$J = J_{SC} - J_0 \left\{ \exp \left[q \left(V + \frac{AJ(V)R_s}{k_B T_a} \right) \right] - 1 \right\} - \frac{V + AJ(V)R_s}{AR_{sh}} \quad (S2)$$

Where J_0 , T_a and A are the dark current density, atmosphere temperature and active area, respectively. The q and k_B are the elemental charge and Boltzmann constant, respectively. When the reduction of leakage current mainly originates from the reduction of R_s , the simulated J-V curve shows a large enhancement of FF without significant changes in J_{SC} and V_{OC} , as shown in Fig. S2B. The simulated results are well matched with our experimental results in **Fig. 1A-C** and Figure S1.

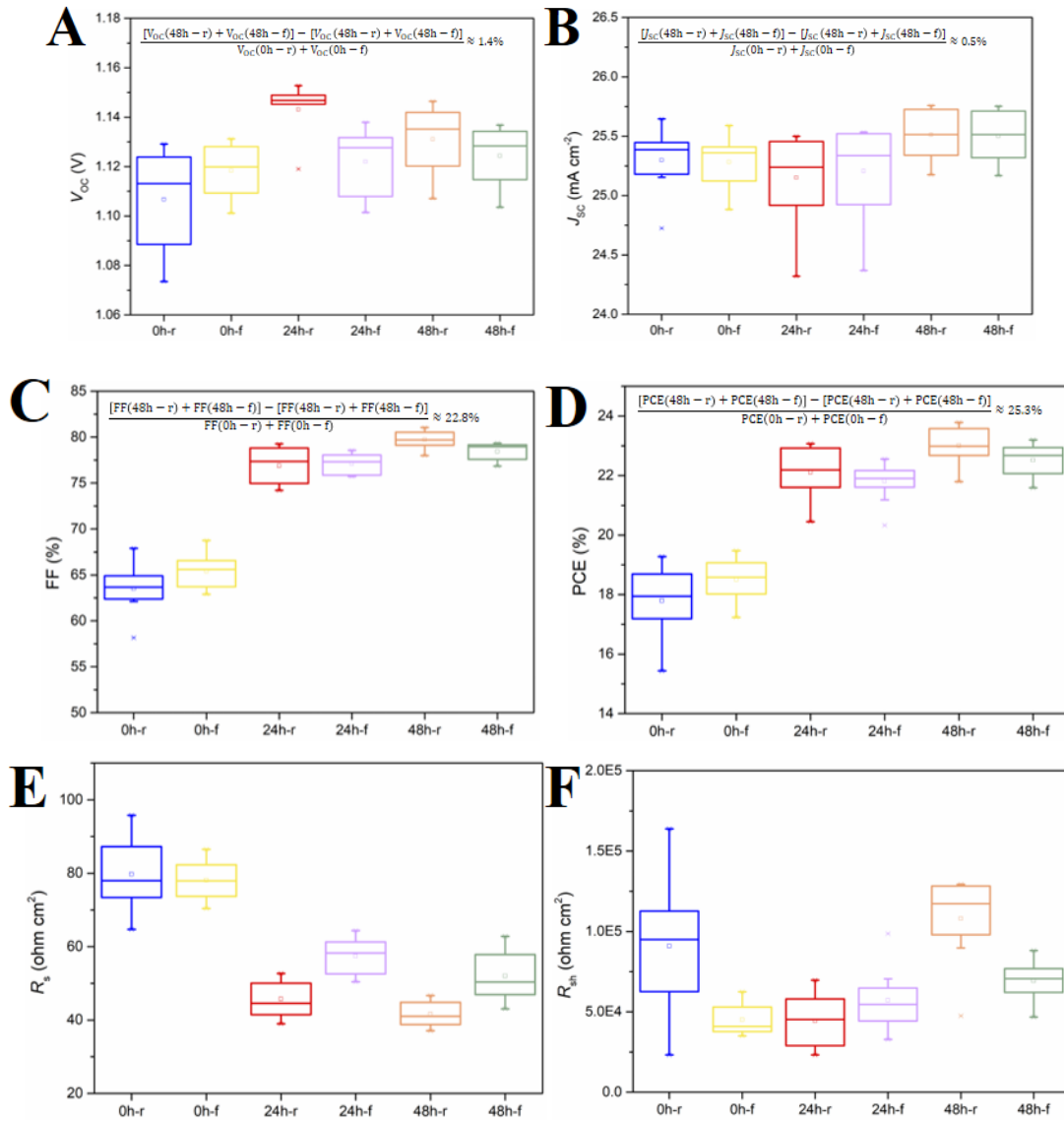


Fig. S1 Original performance evolution of regular Ag-PSCs stored under dark and dry environment. (A) V_{oc} , (B) J_{sc} , (C) FF, (D) PCE, (E) R_s and (F) R_{sh} . Twenty individual PSCs were fabricated, and the -f and -r represent the J-V characterization under forward and reverse scan, respectively

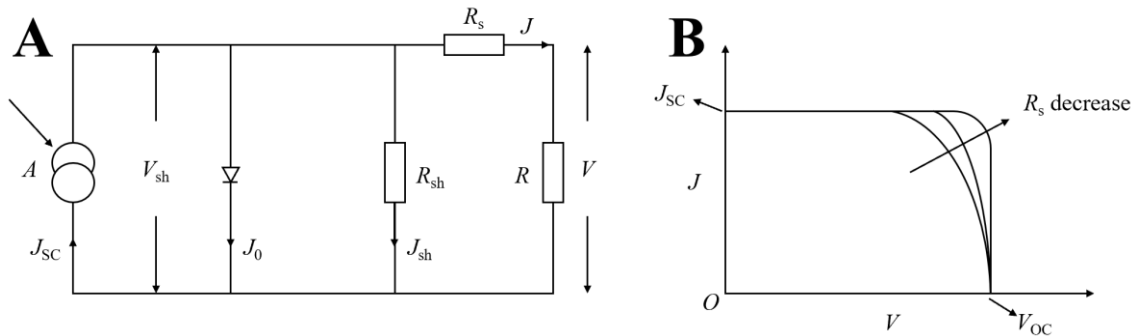


Fig. S2 The Equivalent circuit of a solar cell with parasitic resistance. (A) schematic diagram and (B) the effect of reduction of R_s on the J-V curves. The V_{sh} and J_{sh} is the shunt voltage and shunt current density, respectively

Note S2: The Reason for Selecting (FA,MA)Pb(I,Br)₃ Perovskite System

The similar performance enhancement in FFs was also observed in regular Ag-devices based on (FA,MA)Pb(I,Br)₃, and the critical period for enhancement was also the first 24 h of storage. These phenomena suggest the following points: 1) the efficient regular Ag-PSCs can be realized with various record-maker perovskites; 2) the main reason for the enhancement of FF and PCE should be the self-modification of the adjacent interface of HTM/Ag anode in the first 24 h.

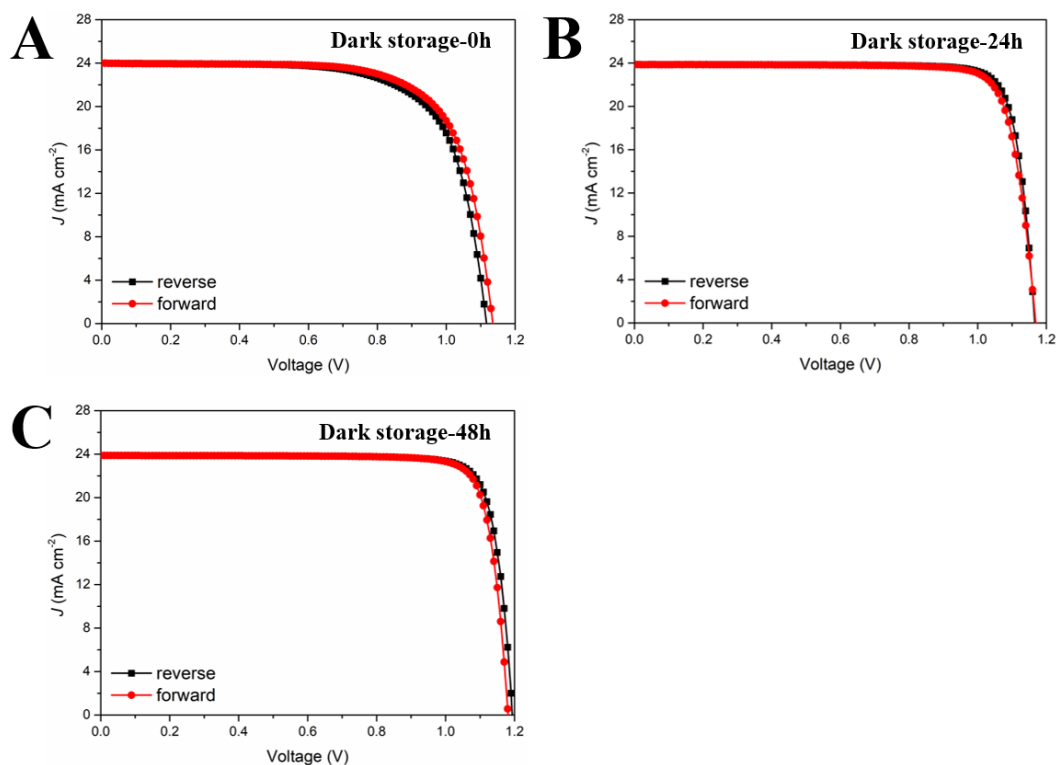


Fig. S3 *J-V* curves of champion regular Ag-PSCs based on (FA,MA)Pb(I,Br)₃ stored under dark and dry environment for varying times. (A) 0h, (B) 24h, and (C) 48h

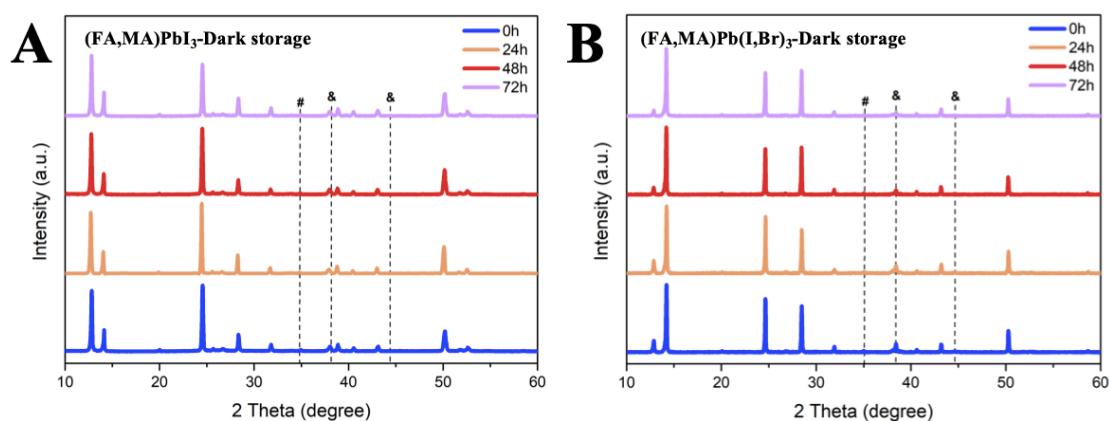


Fig. S4 XRD patterns of perovskite on regular Ag-PSCs stored under dark and dry environment for varying times. (A) (FA,MA)PbI₃ perovskite and (B) (FA,MA)Pb(I,Br)₃ perovskite. Notes that the Ag anode was peeled off by tape. The characteristic peaks of residue AgI and Ag are marked with signature # and &, respectively

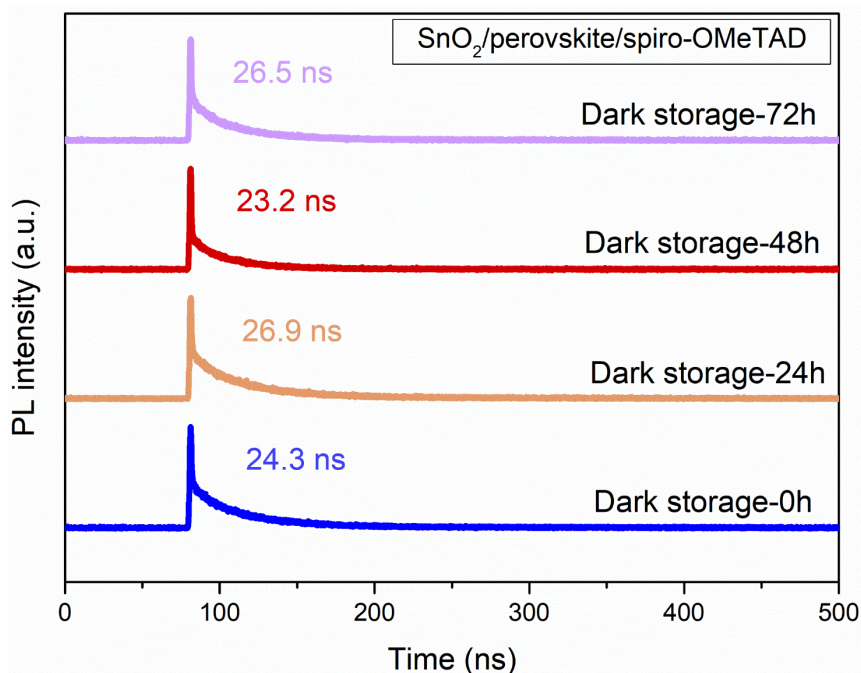


Fig. S5 TRPL results of SnO₂/(FA,MA)PbI₃ perovskite/spiro-OMeTAD bi-interfaces on glass substrates stored under dark and dry environment for varying times

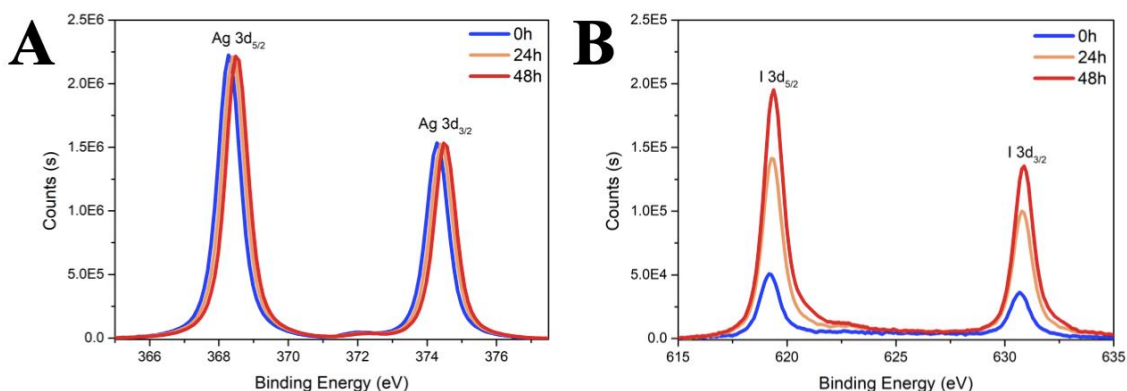


Fig. S6 High-resolution XPS of Ag anode on PSCs stored under dark and dry environment (A) Ag 3d and (B) I 3d core signals

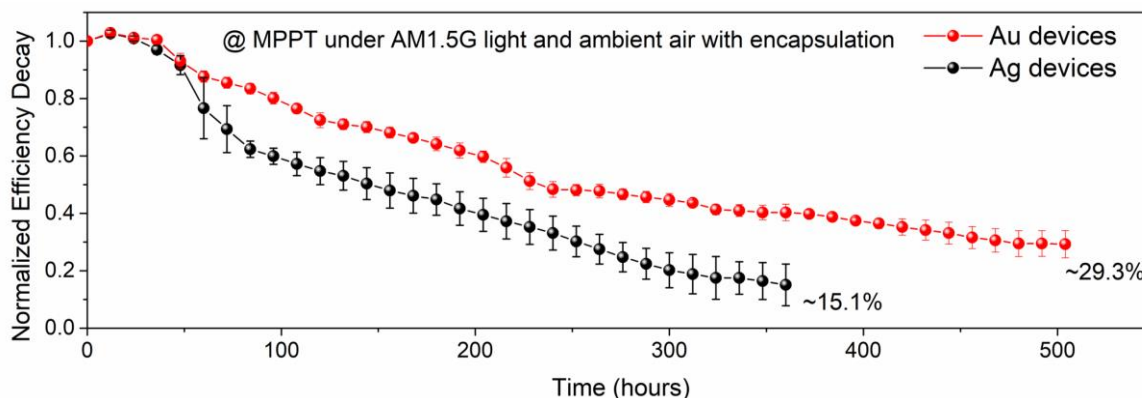


Fig. S7 The operational stability of encapsulated Ag and Au devices at MPP under 1-sun illumination (AM 1.5G, 100 mW cm⁻²) and ambient air. The error bars denote standard deviations for five individual devices

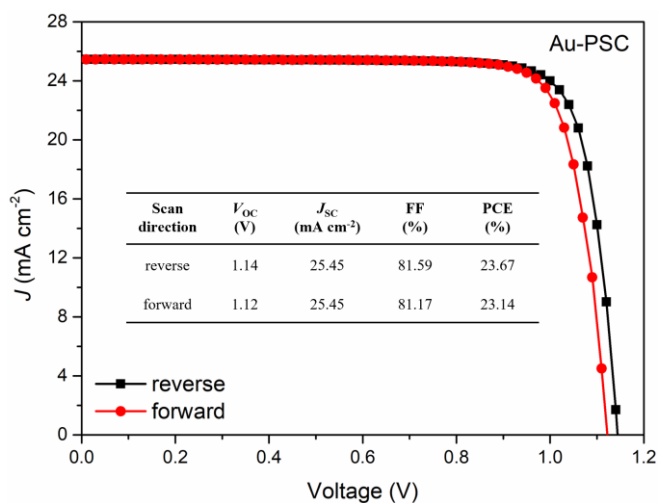


Fig. S8 *J-V* curves of champion regular Au-PSC

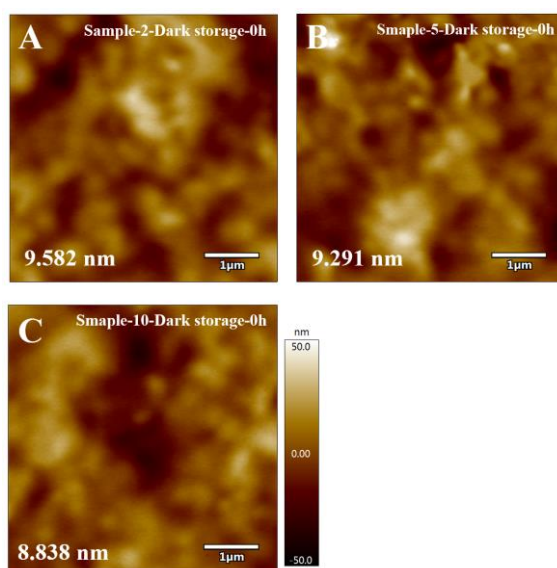


Fig. S9 The xy-plane film morphology of glass/FTO/SnO₂/(FA,MA)PbI₃ perovskite/spiro-OMeTAD/ultrathin Ag layer without storage by depositing (A) 2 nm, (B) 5 nm, and (C) 10 nm, respectively, measured by AFM

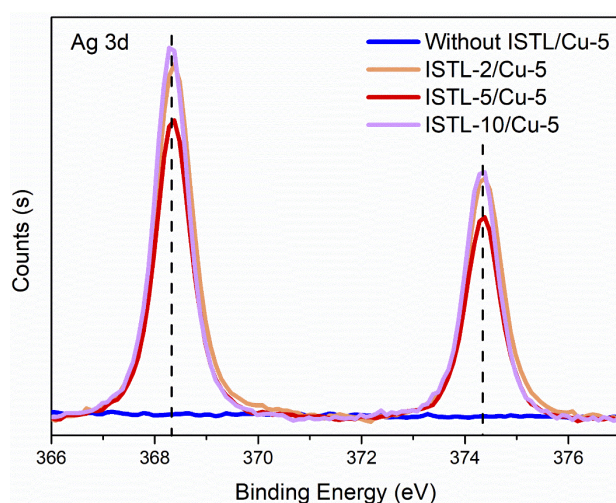


Fig. S10 High-resolution XPS of Ag 3d core levels of the evaporated Ag atop FTO/SnO₂/(FA,MA)PbI₃ perovskite/spiro-OMeTAD after 24-hour storage under dark and dry environment (< 10% relative humidity)

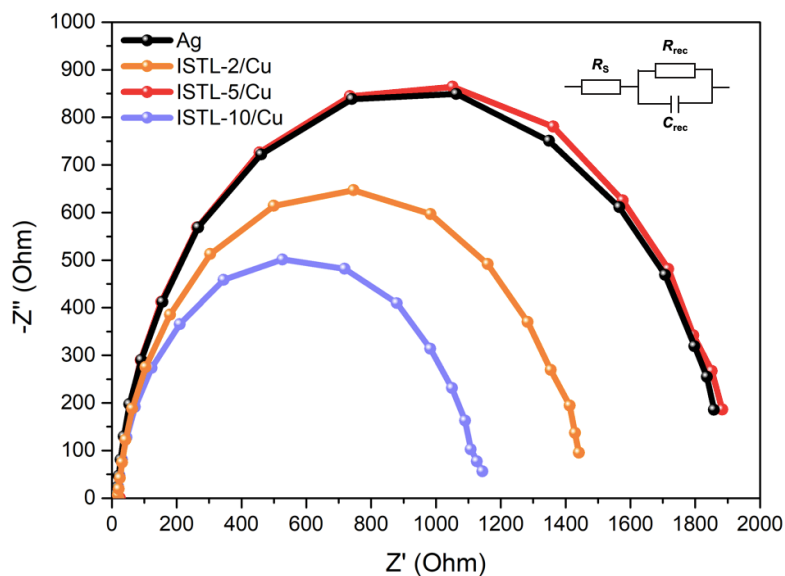


Fig. 11 Nyquist plots of Ag-PSC and Cu-PSCs with different ISTLs in dark condition with 0.9 V bias around 1 Hz to 1 MHz. The equivalent circuit employed to fit the spectra, where R_s is the series resistance and C_{rec} is charge recombination capacitance

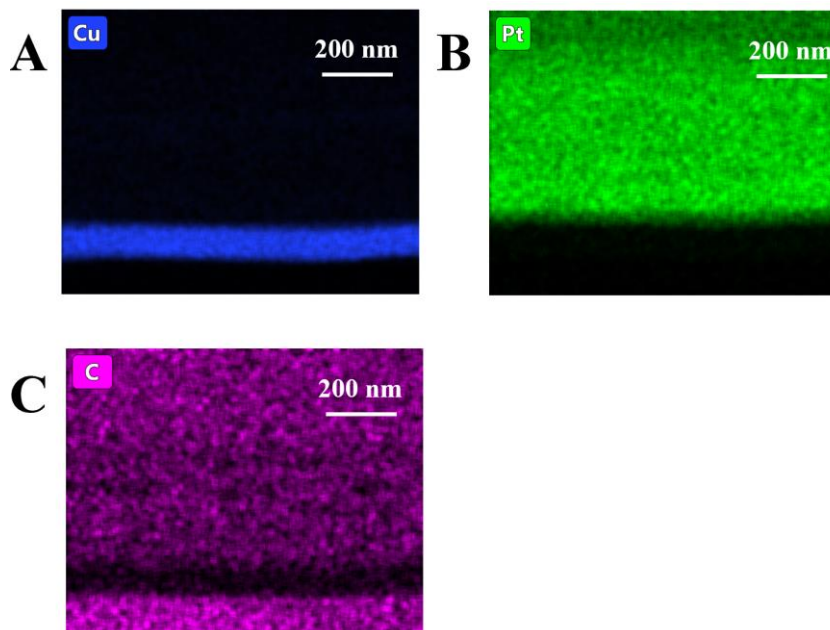


Fig. S12 Element distributions of ISTL-5 in Figure 4B by EDS mapping. (A) Cu element, (B) Pt element and (C) C element

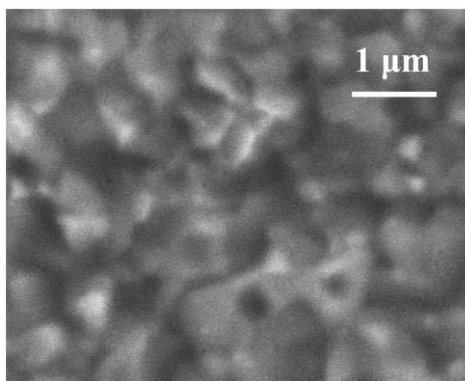


Fig. S13 The top-view SEM image of ISTL-5 atop FTO/SnO₂/(FA,MA)PbI₃ perovskite/spiro-OMeTAD

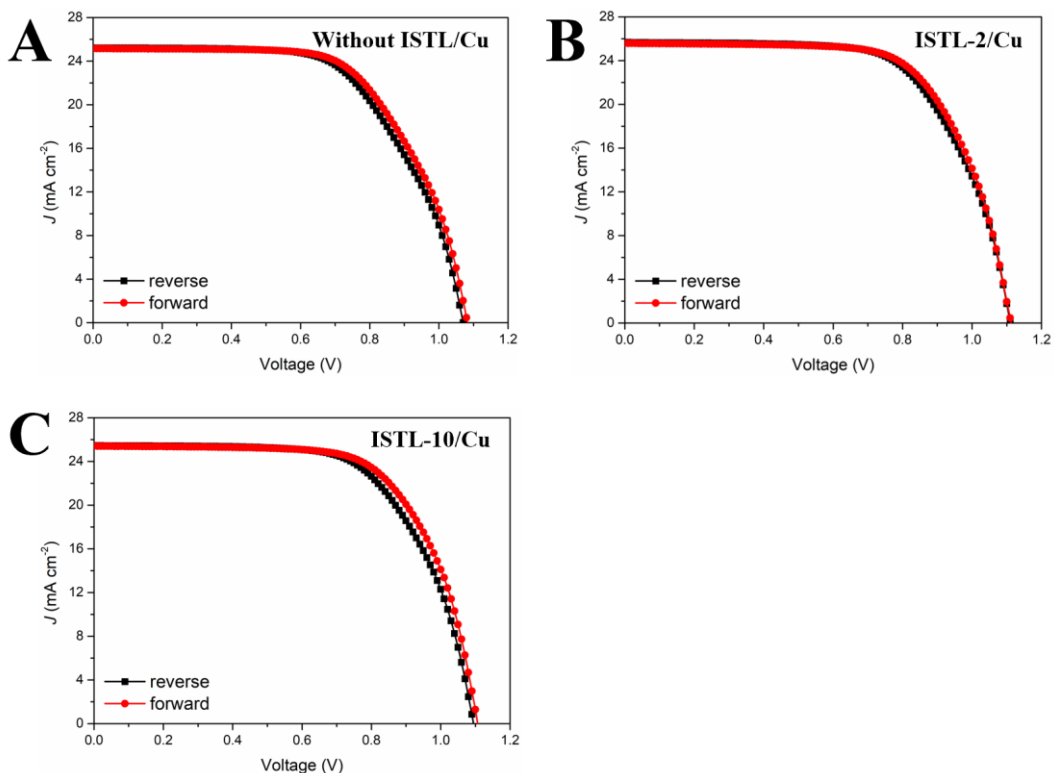


Fig. S14 J-V curves of champion Cu-PSCs (A) without ISTL, (B) with ISTL-2, and (C) with ISTL-10 stored under dark and dry environment for 48h, respectively

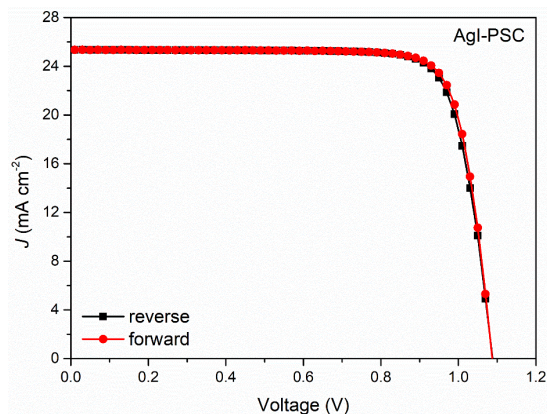


Fig. S15 J-V curves of the champion regular AgI-PSC

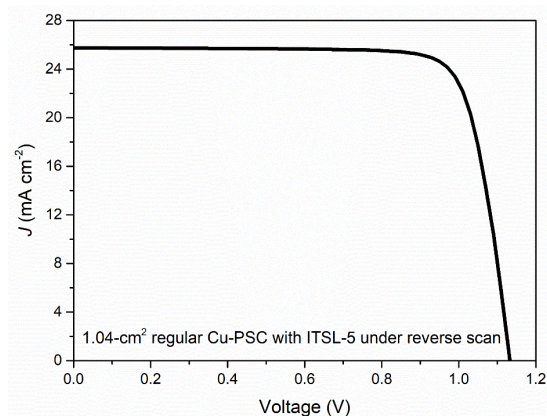


Fig. S16 J-V curves of the champion Cu-PSC with ISTL-5 and an aperture area of 1.04 cm² under reverse scan measured in our lab

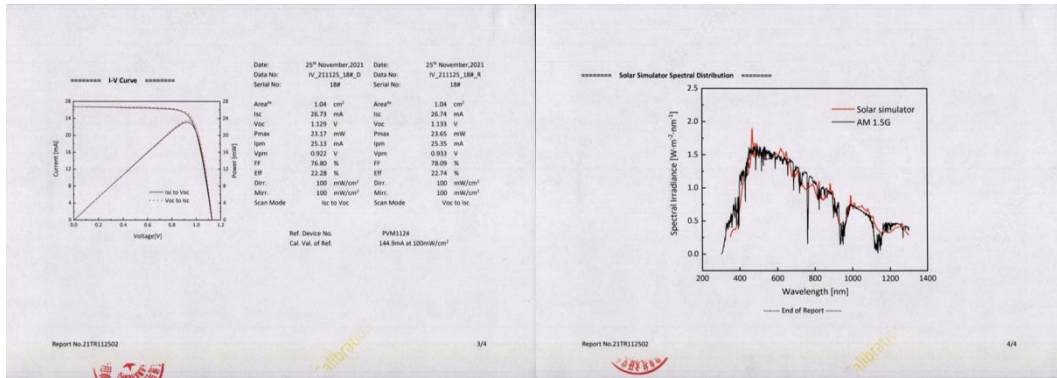
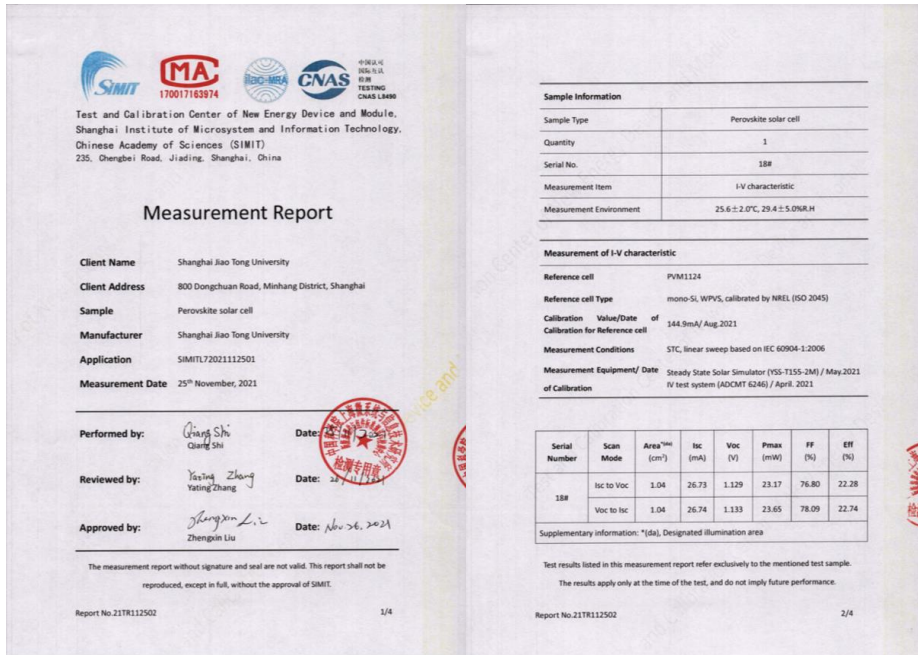


Fig. S17 Certificated results of 1.04-cm² Cu-PSC with ISTL-5 by the Shanghai Institute of Microsystem and Information Technology, Chinese Academy of Science, China (SIMIT, China). The reverse scan is performed from 1.2 V to -0.1 V at 30 mV s⁻¹, with a PCE of 22.74% (V_{OC}=1.133 V, I_{SC}=26.74 mA, FF=78.09%). The forward scan is performed from -0.1 V to 1.2 V at 30 mV s⁻¹, with a PCE of 22.28% (V_{OC}=1.129 V, I_{SC}=26.73 mA, FF=76.80%). The hysteresis index of the device is less than 3%

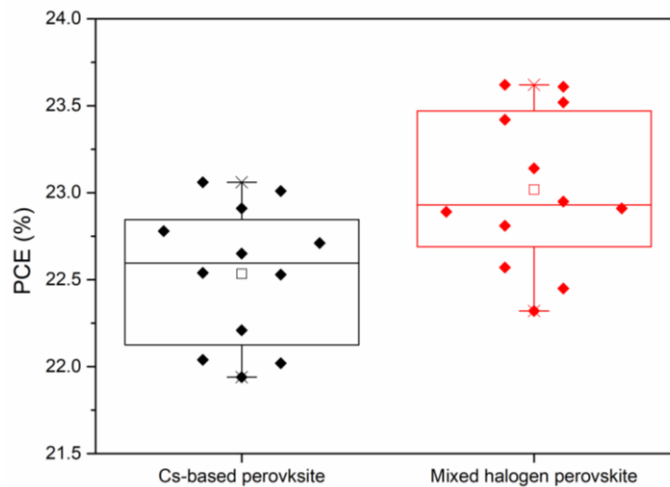


Fig. S18 The box plots of PCE of 0.09-cm² Cu-PSCs with different perovskites stored under dark and dry environment for 48h. The device structure is FTO/SnO₂/perovskite/spiro-OMeTAD/ISTL-5/Cu

Table S1 Performance parameters of champion regular Ag-PSC stored under dark and dry environment for varying times

Dark Storage Time (h)	V _{oc} (V)	J _{sc} (mA cm ⁻²)	FF (%)	PCE (%)	R _s (Ohm cm ²)	R _{sh} (Ohm cm ²)
0-r	1.11	25.37	67.91	19.12	5.18	5617.11
0-f	1.12	25.32	68.76	19.50	5.86	2804.26
24-r	1.15	25.50	79.01	23.17	3.41	5571.82
24-f	1.12	25.52	77.70	22.21	5.06	4187.49
48-r	1.14	25.71	81.04	23.86	2.97	10344.49
48-f	1.12	25.69	79.50	22.87	4.88	5344.84

Table S2 Performance parameters of champion Ag-PSC based on (FA,MA)Pb(I,Br)₃ stored under dark and dry environment for varying times

Dark Storage Time (h)	V _{oc} (V)	J _{sc} (mA cm ⁻²)	FF (%)	PCE (%)	R _s (Ohm cm ²)	R _{sh} (Ohm cm ²)
0-r	1.12	24.00	69.91	18.79	3.92	4758.80
0-f	1.13	23.98	70.81	19.19	3.77	3284.07
24-r	1.17	23.88	83.32	23.28	2.15	16787.16
24-f	1.17	23.85	81.84	22.84	2.84	26826.16
48-r	1.19	23.87	83.33	23.67	1.90	18440.14
48-f	1.18	23.87	83.44	23.51	2.17	18097.96

Table S3 The estimated t_{ave} of iodine ions through spiro-OMeTAD HTMs with a thickness ranging from 100 nm to 300 nm

The thickness of spiro-OMeTAD HTM (nm)	Estimated t _{ave} (hour)
100	0.031
150	0.070
200	0.124
250	0.195
300	0.280

Table S4 Performance parameters of champion Cu-PSCs without ISTL or with different thickness of ISTLs stored under dark and dry environment for 48h

Sample	V _{oc} (V)	J _{sc} (mA cm ⁻²)	FF (%)	PCE (%)	R _s (Ohm cm ²)	R _{sh} (Ohm cm ²)
Without ISTL/Cu-r	1.07	25.21	62.12	16.76	6.63	13106.25
Without ISTL/Cu-f	1.08	25.15	63.45	17.23	6.50	4997.98
ISTL-2/Cu-r	1.11	25.66	65.41	18.63	5.83	7053.58
ISTL-2/Cu-f	1.11	25.58	66.71	18.94	5.93	3036.72
ISTL-5/Cu-r	1.11	25.68	82.95	23.64	2.30	32120.48
ISTL-5/Cu-f	1.11	25.69	82.36	23.51	2.20	20572.67
ISTL-10/Cu-r	1.09	25.45	64.40	17.86	5.91	8150.05
ISTL-10/Cu-f	1.11	25.41	66.42	18.73	5.63	3388.79

Table S5 Performance parameters of champion Cu-PSC with ISTL-5 stored under dark and dry environment for varying times

Dark Storage Time (h)	V _{oc} (V)	J _{sc} (mA cm ⁻²)	FF (%)	PCE (%)	R _s (Ohm cm ²)	R _{sh} (Ohm cm ²)
0-r	1.09	25.72	81.58	22.87	2.90	35794.66
0-f	1.08	25.69	80.59	22.36	2.01	12564.78
24-r	1.11	25.69	82.16	23.43	2.30	17414.20
24-f	1.10	25.70	81.16	22.94	2.12	10683.22
48-r	1.11	25.68	82.95	23.64	2.30	32120.48
48-f	1.11	25.69	82.36	23.51	2.20	20572.67

Table S6 Performance parameters of champion regular PSCs with other ISTLs or low-WF anodes stored under dark and dry environment for 48h

Sample	V _{oc} (V)	J _{sc} (mA cm ⁻²)	FF (%)	PCE (%)
ISTL-CdI ₂ /Cu-r	1.08	25.07	81.63	22.10
ISTL-CdI ₂ /Cu-f	1.08	25.06	80.25	21.72
ISTL-SnI ₄ /Cu-r	1.10	25.06	80.05	22.07
ISTL-SnI ₄ /Cu-f	1.09	25.07	78.73	21.51
ISTL-AgI/Ti-r	1.10	25.02	80.04	22.03
ISTL-AgI/Ti-f	1.09	25.01	78.25	21.33
ISTL-AgI/Al-r	1.09	25.22	80.21	22.05
ISTL-AgI/Al-f	1.07	25.24	78.43	21.18